Chemical Science

ROYAL SOCIETY OF CHEMISTRY

EDGE ARTICLE

View Article Online
View Journal | View Issue

Cite this: *Chem. Sci.*, 2023, **14**, 11365

All publication charges for this article have been paid for by the Royal Society of Chemistry

Received 22nd May 2023
Accepted 28th August 2023

DOI: 10.1039/d3sc02590j

rsc.li/chemical-science

Mild and scalable synthesis of phosphonorhodamines†

Joshua L. Turnbull,[a] Ryan P. Golden,[a] Brittany R. Benlian,[b] Katharine M. Henn,[c] Soren M. Lipman [a] and Evan W. Miller *[abc]

Since their discovery in 1887, rhodamines have become indispensable fluorophores for biological imaging. Recent studies have extensively explored heteroatom substitution at the 10′ position and a variety of substitution patterns on the 3′,6′ nitrogens. Although 3-carboxy- and 3-sulfono-rhodamines were first reported in the 19th century, the 3-phosphono analogues have never been reported. Here, we report a mild, scalable synthetic route to 3-phosphonorhodamines. We explore the substrate scope and investigate mechanistic details of an exogenous acid-free condensation. Tetramethyl-3-phosphonorhodamine (phosTMR) derivatives can be accessed on the 1.5 mmol scale in up to 98% yield (2 steps). phosTMR shows a 12- to 500-fold increase in water solubility relative to 3-carboxy and 3-sulfonorhodamine derivatives and has excellent chemical stability. Additionally, phosphonates allow for chemical derivatization; esterification of phosTMR facilitates intracellular delivery with localization profiles that differ from 3-carboxyrhodamines. The free phosphonate can be incorporated into a molecular wire scaffold to create a phosphonated rhodamine voltage reporter, phosphonoRhoVR. PhosRhoVR 1 can be synthesized in just 6 steps, with an overall yield of 37% to provide >400 mg of material, compared to a 6-step, ~2% yield for the previously reported RhoVR 1. PhosRhoVR 1 possesses excellent voltage sensitivity (37% $\Delta F/F$) and a 2-fold increase in cellular brightness compared to RhoVR 1.

Introduction

Small molecule fluorophores have revolutionized our ability to visualize complex biological systems.[1,2] Biological imaging modalities rely on access to fluorophores with high brightness, stability, and water solubility. Rhodamines, the amino isologues of fluoresceins, find widespread use in bioimaging applications. In comparison to fluoresceins, rhodamines are insensitive to pH, exhibit improved photostability, and have tunable excitation and emission across the visible spectrum.[3]

Modification of the structure of rhodamines can produce dramatic changes in the functional properties of the dyes (Scheme 1). Changing the alkylation pattern on the 3′ and 6′ amines tunes absorption and emission wavelengths,[4] fused cyclohexanes or 4-membered azetidine rings improve brightness,[5] and heteroatom substitution of the 10′ oxygen atom results in a red shift.[6–14] Additionally, the delocalized positive charge of rhodamine facilitates cell permeability, making rhodamines attractive scaffolds for intracellular or live-cell imaging applications.[15]

Substitutions of the rhodamine core have been extensively explored for the modulation of photophysical properties. On the other hand, substitutions at the 3-position of the pendant aryl ring – which include carboxylates, amides, sulfonates, methyl, and substituted methylenes – largely impact subsequent applications of rhodamine fluorophores. We recently disclosed a new class of fluoresceins with 3-phosphonate substitutions. 3-Phosphonofluoresceins exhibit an almost 2-fold improvement in water solubility compared to 3-carboxy analogs,[16] and functionalization of the 3-phosphonate with esters improves cellular brightness 70-fold over traditional 3-carboxyfluorescein. Owing to the orthogonality of the xanthene core and the pendant ring, physical changes brought by 3-phosphonate substitution were facilitated without compromising brightness or excitation/emission wavelengths. Expansion of 3-phosphonate

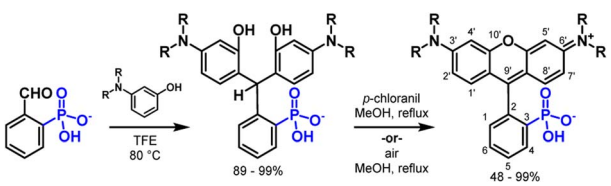

Scheme 1 Mild synthesis of phosphonorhodamines.

[a]Department of Chemistry, University of California, Berkeley, CA, 94720-1460, USA. E-mail: evanwmiller@berkeley.edu

[b]Department of Molecular & Cell Biology, University of California, Berkeley, CA, 94720-1460, USA

[c]Helen Wills Neuroscience Institute, University of California, Berkeley, CA, 94720-1460, USA

† Electronic supplementary information (ESI) available. See DOI: https://doi.org/10.1039/d3sc02590j

substitution to rhodamines may yield additional opportunities in the applications of xanthene fluorophores.

Despite almost 140 years since the first rhodamine was synthesized, synthetic approaches often lack generalizability with respect to varying 3-substitution. In fact, rhodamines are largely constructed by variations of the initially reported Friedel–Crafts condensation.[17,18] Phthalic anhydrides are heated with aminophenols in the presence of Brønsted or Lewis acids; however, functionalized phthalides often lead to mixture of regioisomers that are difficult to separate.[19] To solve this problem, benzaldehydes can be condensed with aminophenols followed by dehydration and *in situ* oxidation with exposure to air or use of an organic oxidant such as chloranil.[18] The harsh nature of these condensations often results in low yields, functional group incompatibility and troublesome purifications.[1,20,21] While the acidic conditions present in all of these reaction schemes increase reactivity of the electrophile, protonation, or Lewis acid complexation, with the aniline decreases the nucleophilicity of aminophenols. An elegant recent example showed that intramolecular activation of the benzaldehyde by an *ortho* carboxylic acid could furnish rhodamines in high yields without the addition of an acid catalyst.[22]

Contemporary methods to access rhodamines make use of Pd-catalyzed C–N cross coupling of fluorescein ditriflates with various amines,[23] addition of aryl organometallic species into *N*-alkylated diaminoxanthones,[24,25] or addition of dimetallated bisphenyl ethers into electrophiles such as aryl esters or phthalic anhydrides.[10,26] While these methods alleviate some of the challenges associated with classic rhodamine condensations, their applications to the synthesis of rhodamines with acidic 3-functionalities (such as phosphonates) are limited.

Here, we report a mild synthesis of 3-phosphonorhodamines in exceptional yields from the condensation of aminophenols and 2-phosphonobenzaldehyde (Scheme 1). 3-Phosphonorhodamines can be synthesized on a 1.5 mmol scale, often without the need for chromatography, alleviating many of the challenges associated with purification of charged fluorophores. The 3-phosphonorhodamines have nearly identical optical properties compared to their classic 3-carboxy- and sulfono-counterparts but possess a >10- to 500-fold increase in water solubility. The tetramethyl-substituted 3-phosphonorhodamine can be applied to diverse cellular imaging contexts. First, esterification of the phosphonate controls cellular localization, and tetramethylphosphonorhodamine shows enhanced cellular brightness compared to the analogous 3-carboxyrhodamine. Next, 3-phosphonorhodamines can be localized to plasma membranes and used for voltage imaging, where they show comparable voltage sensitivity and a 2-fold increase in cellular brightness compared to carboxy-based indicators.

Results and discussion

Synthesis of 3-phosphonorhodamines

The key role of acid in the Friedel–Crafts condensations of xanthene fluorophores, such as rhodamines, is to activate the aldehyde and promote nucleophilic attack from electron rich arenes. In the case of 2-carboxybenzaldehyde, the acidic nature of the *ortho* carboxylate provides intramolecular activation of the aldehyde, increasing electrophilicity.[27] The intramolecular activation is evident through slight formation (13%) of the corresponding hemiacetal in alcoholic solvents such as CD_3OD (Table S1 and Scheme S1†). Dwight and Levin previously reported a relatively mild, acid-free synthesis of 3-carboxyrhodamines that is mediated by this phenomenon of intramolecular activation.[22]

By analogy to this previous report,[22] acidic phosphonates may equip 2-phosphonobenzaldehyde (**1**) with similar intramolecular aldehyde activation and provide a path to 3-phosphonorhodamines in the absence of exogenous acid. This is the case. Heating of **1** with 3-(dimethylamino)phenol, **2**, in 2,2,2-trifluoroethanol (TFE) results in clean precipitation of triarylmethane **9** in an excellent 98% yield. **9** can be isolated by precipitation and undergoes quantitative dehydration and oxidation to the corresponding rhodamine **16** (Scheme 2).

In previous studies, the analogous reaction with 2-carboxybenzaldehyde required TFE to achieve appreciable yields.[22] This is likely a result of stabilization of the benzhydrilium intermediate by the high ionizing power, low nucleophilicity, and hydrogen bond donating ability of fluorinated alcohols (such as TFE) compared to hydrocarbon-based alcohols.[22,28–30] As in previous studies,[22] the reaction between **1** and **2** in TFE produces **9** in high yields (Scheme 3 and Table 1). However, the reaction of **1** and **2** in methanol also produces **9** in moderate yield (up to 58%, Scheme 3 and Table 1). This increased reactivity is likely a result of the greater extent of intramolecular activation of aldehyde **1** compared to 2-carboxybenzaldehyde. NMR studies support this hypothesis: 2-phosphonobenzaldehyde (**1**) shows a greater propensity to form the corresponding hemiacetal in nucleophilic solvents such as CD_3OD (Table S1 and Scheme S1†). Aryl phosphonates generally have pK_{a1} values that are about 2 pH units lower than the corresponding benzoic acid pK_a.[31] The low pK_a of the phosphonate may also contribute to greater stabilization of the benzhydrilium intermediate.

To examine the generalizability of this synthetic approach, we exposed aldehyde **1** to a series of anilines, **2** to **7**, under the same conditions (TFE, 80 °C, 16 hours) and observe precipitation of triarylmethanes **9** to **14** in excellent yields, ranging from 89 to 99% (Table 1). The exceptional yields of **9** to **14** are likely due in part to the insolubility of the triarylmethanes in alcoholic solvents. Friedel–Crafts condensations are reversible, as

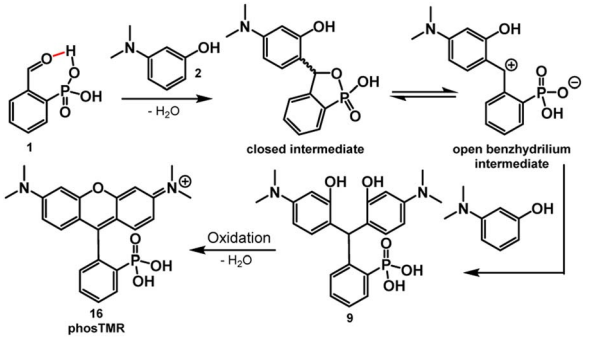

Scheme 2 Stepwise formation of phosTMR.

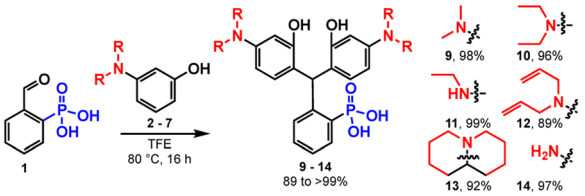

Scheme 3 Synthesis of triarylmethane intermediates.

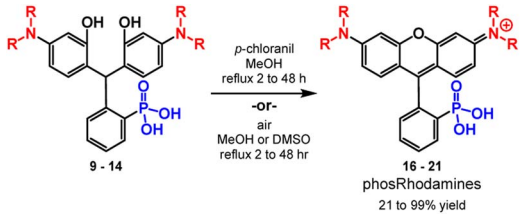

Scheme 4 Synthesis of phosphonorhodamines.

Table 1 Synthesis of triarylmethane intermediates

	Aniline	Product	Conditions	Yield[a]
2	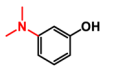	**9**	TFE, 80 °C, 16 h[b] MeOH, 60 °C, 16 h MeOH, rt, 16 h	98% 58% 22%
3	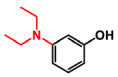	**10**	TFE, 80 °C, 16 h MeOH, rt 16 h	96% 27%
4	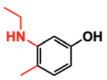	**11**	TFE, 80 °C, 16 h	99%
5	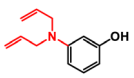	**12**	TFE 80 °C, 16 h[b]	89%
6	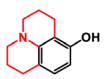	**13**	TFE, 80 °C, 16 h[b] MeOH, rt, 16 h	92% 65%
7	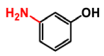	**14**	TFE, 80 °C, 16 h	97%

[a] Isolated yields. [b] Performed under a nitrogen atmosphere.

evidenced by the degradation of the triarylmethane intermediates in the presence of acid.[32] Precipitation from the reaction medium drives reaction progression and contributes to the near quantitative yields. For more soluble intermediates, like **13**, performing the reaction under an inert atmosphere improves the yield, by avoiding premature oxidation to the final rhodamine, which would otherwise complicate purification at this stage (Table 1).

Some substrates are not compatible with this methodology. Reaction of **1** with resorcinols does not yield the corresponding phosphonofluorescein. Instead, the reaction produces just a single addition of resorcinol to **1**. Electron-rich anilines may be required to stabilize the benhzydrilium intermediate and promote a 2nd Friedel–Crafts addition (Scheme 2).

Further, azetidines are not currently compatible. Alcoholic solvents promote cationic ring opening polymerization of azetidines.[33] Use of azetidine-substituted aminophenol **8** – which would provide a mild route to phosphono JaneliaFluor intermediate **15** – gives an intractable solid precipitate under our current reaction conditions (Scheme S2†).

After isolating triarylmethane intermediates **9** to **14** in high yields and purity, we examined conditions for the dehydration and oxidation to the corresponding 3-phosphonorhomdamines **16** to **21** (Scheme 4).

In most cases, reflux in methanol with *p*-chloranil as an oxidant leads to cyclization and oxidation to the corresponding rhodamine. As dehydration and oxidation to the rhodamines occurs, solubility in methanol increases and so reaction progression can be easily monitored by the dissolution of visible particulates. Reaction times vary from 2 to 48 hours and depend on the volume of methanol used. Upon completion, filtration removes any unoxidized fluorophore and trituration with organic solvent to remove excess chloranil yields rhodamines **16** to **19** in excellent yields (80–99%, Table 2) without need for further purification. Substrates **13** and **14** are sensitive to chloranil oxidation, leading to decomposition. Instead, reflux in methanol or DMSO with exposure to air is sufficient to promote dehydration and oxidation to rhodamines **20** and **21** respectively; however, these methods require purification by reverse phase silica chromatography. The dehydration and oxidation of **14** to phosRho110, **21**, is particularly low yielding (21%), owing to the limited solubility of the fluorophore and challenging purification. An alternative synthesis through de-allylation of **19** (Scheme S3†) gives **21** in 71% yield (Table S2†).

Finally, condensation of aminophenols with phosphonate monoesters are also compatible with this reaction methodology. Condensation of phosphonate monoester **22** with **2**, followed by dehydration and chloranil oxidation affords rhodamine **23** in 39% yield with the ethyl ester intact (Scheme 5). Although a reduced yield compared to the 98% for **16**, these results show that monoesters possess the ability to facilitate the reaction *via* intramolecular activation of the aldehyde. Importantly the strongly acidic conditions typically required for these condensations would result in phosphonate ester hydrolysis and thus the direct synthesis of monoester **23** is a testament to the mild nature of this chemistry. The reaction of **2** with the diethylester of **1** gives no reaction in TFE or MeOH.

The conditions used to achieve high yields of phosphonorhodamines do not translate to high yields for 2-carboxy and 2-sulfono rhodamines. While 2-carboxybenzaldehyde also provides intramolecular activation,[22,27] reaction with **2** under the same conditions produces carboxyTMR in only 31% yield and requires chromatography (ESI†). This represents more than a 3-fold decrease in the yield compared to phosTMR, **16**. The lower pK_a of arylphosphonates compared to benzoic acids may account for the differing reactivity. On the other hand, 2-sulfonobenzaldehyde does not produce sulfoTMR under these conditions, suggesting the pK_a of the arylsulfonic acid is too low and therefore has no proton to activate the aldehyde. As such, sulfoTMR was synthesized by heating with **2** in neat methanesulfonic acid in just 12% yield (ESI†).

Table 2 Synthesis of phosphonorhodamines

Triarylmethane	Rhodamine	Yield[a]	Conditions
9	**16** phosTMR	99%	*p*-Chloranil, MeOH, reflux, 2–48 h
10	**17** phosRhoB	80%	*p*-Chloranil, MeOH, reflux, 2–48 h
11	**18** phosRho6G	82%	*p*-Chloranil, MeOH, reflux, 2–48 h
12	**19** phosTAR	93%	*p*-Chloranil, MeOH, reflux, 2–48 h
13	**20** phosJulR	48%[b]	MeOH, reflux, 48 h
14	**21** phosRho110	21%[b,c]	DMSO, 100 °C, 12 h

[a] Isolated yields. [b] After reverse phase silica chromatography. [c] **21** is also accessible by deallylation of **19** in up to 71% yield.

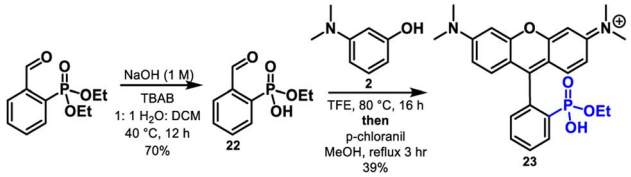

Scheme 5 Direct synthesis of a functionalized phosTMR.

Spectroscopic characterization of 3-phosphonorhodamines

The spectroscopic properties of phosTMR, **16** and the ethyl ester analog phosTMR·OEt, **23** are similar compared to sulfo- and carboxyTMR (Fig. 1a–d and Table 3). Compound **16**, phosTMR, displays a small hypsochromic shift (546/564 nm), relative to carboxyTMR (549/569 nm) in phosphate buffered saline (PBS, pH 7.4). On the other hand, phosTMR·OEt (**23**) has a slight bathochromic shift in absorbance and identical emission (551/569 nm) to carboxyTMR. SulfoTMR absorbs at 556 nm and emits at 574 nm. 3-Substituents have little effect on the spectral profiles of tetramethylrhodamines. The small wavelength shifts (~10 nm) are explained by inductive differences of the pendant ring that arise from these substitutions. Extinction coefficients, Stokes shifts and quantum yields all display little variance in response to 3-substitution owing to the maintained orthogonality of the xanthene chromophore and pendant rings (Table 3).

3-phosphonorhodamine **16** has substantially improved water solubility (12 mM, PBS) compared to sulfono- and carboxyTMR (Fig. S1†). **16** is ~500× more soluble than

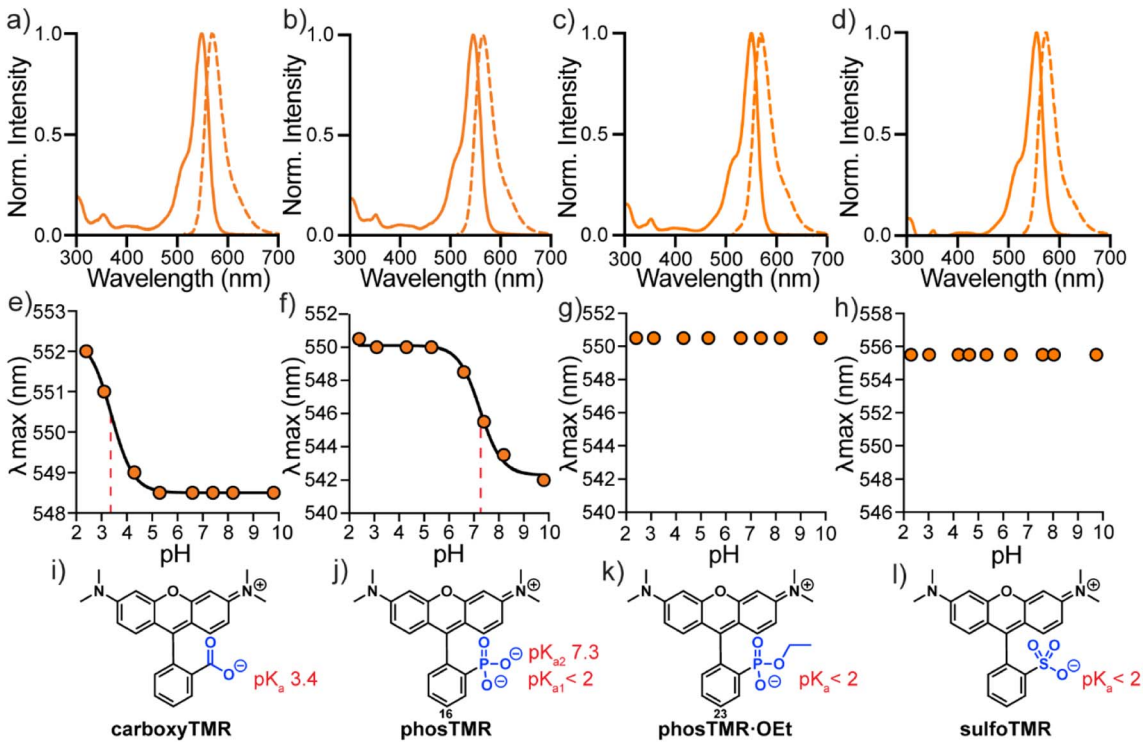

Fig. 1 Spectroscopic characterization of tetramethylrhodamines. Normalized absorbance and fluorescence spectra (a–d) in PBS, plots of λ_{max} *vs.* pH (e–h) and corresponding chemical structures (i–l) for carboxyTMR (a, e and i), phosTMR (b, f and j), phosTMR·OEt (c, g and k) and sulfoTMR (d, h and l). pH titrations were performed in 10 mM buffered solutions (see ESI†) containing 150 mM NaCl ranging from pH 2.3 to 9.8 at a final dye concentration of 2 μM. Where applicable, titration curves were fit to sigmoidal dose response curves (solid black) to enable pK_a determination (dashed red). Determined pK_a values are reported next to chemical structures (i–l).

Table 3 Properties of rhodamines

Rhodamine	λ_{max}[a]/nm	λ_{em}[a]/nm	ε[a,b]/M^{-1} cm^{-1}	Φ[a]	Solubility[c] (mM)
carboxyTMR	549	569	78 000	0.45	0.9 ± 0.02
sulfoTMR	556	574	73 000	0.46	0.02 ± 0.002
phosTMR, **16**	546	564	70 000	0.52	12 ± 0.6
phosRhoB, **17**	553	570	75 000	0.38	—
phosRho6G, **18**	520	539	76 000	0.95	—
phosTAR, **19**	540	559	53 000	0.68	—
phosJulR, **20**	573	591	91 000	0.99	—
phosRho110, **21**	495	515	76 000	0.98	—
phosTMR·OEt, **23**	551	569	78 000	0.51	—

[a] Measured in PBS. [b] At maximum absorption. [c] Measured in PBS, values are mean ± standard deviation.

sulfonoTMR (0.02 mM) and ∼12× more soluble than carboxyTMR (0.9 mM) (Table 3). This is a larger improvement in solubility than phosphonofluorescein, which is ∼2× more soluble than the related carboxyfluorescein.[16] While fluorescein solubility correlates well with the 3-functionality pK_a, relative solubility of rhodamines appear more nuanced. In the absence of the negatively charged phenolate of fluoresceins, 3-substituents of rhodamines seem to have a greater impact on relative solubility. Improved water solubility will be a boon for applications where removal of residual fluorophore is important to improve contrast, for example, *in vitro* protein labelling or next generation sequencing.[34–36] 3-Phosphonorhodamine **16** shows exceptional stability compared to carboxyTMR. After 1 year of storage as a solid powder, under identical conditions, (at room temperature, 15–22 °C, in the dark), carboxyTMR decomposed into a complex mixture of compounds, including a substantial amount of aniline demethylation (Fig. S2†). However, phosTMR showed no signs of degradation (Fig. S3†).

The absorbance intensity of 3-phosphonorhodamines **16**, **17**, **18**, **19**, **20**, **21**, and **23** at their respective λ_{max} values are all insensitive to pH changes between pH 2 and 10 (Fig. S4†). The λ_{max} values of carboxyTMR and phosTMR shift by 3.5 and 8 nm, respectively, as pH decreases (Fig. 1e and f). Protonation of the 3-substituent results in more electron-withdrawing inductive character of the pendant ring – giving a red-shift in absorbance, as predicted by the Dewar–Knot rules.[37,38] Fitting the value of λ_{max} to non-linear sigmoidal curves reveals a 3-carboxylate pK_a of 3.4 and 3-phosphonate pK_{a2} of 7.3. Neither phosTMR·OEt nor sulfoTMR show a shift in absorbance wavelength λ_{max} across this pH range, indicating their pK_a values are below 2 (Fig. 1g and h).

All new 3-phosphonorhodamines, **16–21**, **23** (Table 3), show characteristic rhodamine absorbance and emission spectra (Fig. S4†). As expected, changing the alkylation pattern of the anilines results in spectral tuning of the absorption and emission wavelengths from 495/515 nm (**21**) to 573/591 nm (**20**). The absorption intensity of all 3-phosphonorhodamines is insensitive to pH (between 2 and 10) and phosphonate pK_{a2} values range from 7.2 to 7.6 (Fig. S4a–r†). The photostabilities of **16**, carboxyTMR, and sulfoTMR are indistinguishable from one another (Fig. S4v–x†).

Tunable cellular localization of phosTMRs

Biologically labile acetoxy methyl (AM) esters are commonly used to mask anionic functionalities, such as phosphonates, to facilitate cell permeability.[39–41] The AM ester masking strategy can deliver 3-phosphonofluoresceins into cells, where hydrolysis by intracellular esterases releases the phosphonic acid, trapping the fluorophore in the cytosol.[16] We hypothesized that a similar AM ester masking strategy could be exploited to deliver phosTMRs into cells.

Treatment of phosTMR **16** with either ethyl bromide or bromomethyl acetate with the presence of Ag(I) in MeCN yields esterified phosTMRs **24** and **25** in 22% and 25% yield respectively (Scheme 6). Acetoxymethyl esters are prone to hydrolysis by cellular esterases, and upon *in vitro* incubation with porcine liver esterase (PLE), both carboxyTMR AM and phosTMR AM, **25**, show complete hydrolysis to the corresponding carboxyTMR and phosTMR (Fig. S5 and S6†). In the absence of PLE, carboxyTMR AM shows low levels of hydrolysis, while phosTMR AM **25** shows about ∼50% hydrolysis to the phosphonate monoAM ester (Fig. S5 and S6†). Diethyl ester phosTMR·2OEt **24** is resistant to hydrolysis in the presence or absence of PLE (Fig. S7†).

The identity of the phosphonate ester profoundly affects cellular localization of phosphonorhodamines. Both phosTMR **16** and monoester phosTMR·OEt **23** show negligible cellular fluorescence, since the doubly- and singly-ionized phosphonates preclude entry into cells (Fig. 2a and b). However, diesters **24** (ethyl ester) and **25** (AM ester) exhibit strong cellular fluorescence. phosTMR·2OEt **24** exhibits heterogeneous cellular localization (Fig. 2c), which appears to co-localize to mitochondria (Fig. S8†), as expected for rhodamine esters.[15]

On the other hand, the more labile phosTMR AM **25** displays more uniform cytosolic localization compared to either

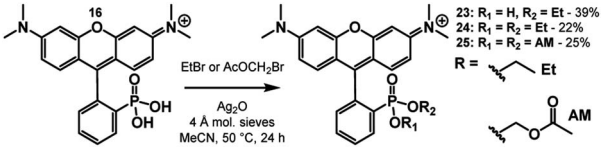

Scheme 6 Synthesis of phosTMR diesters 24 and 25.

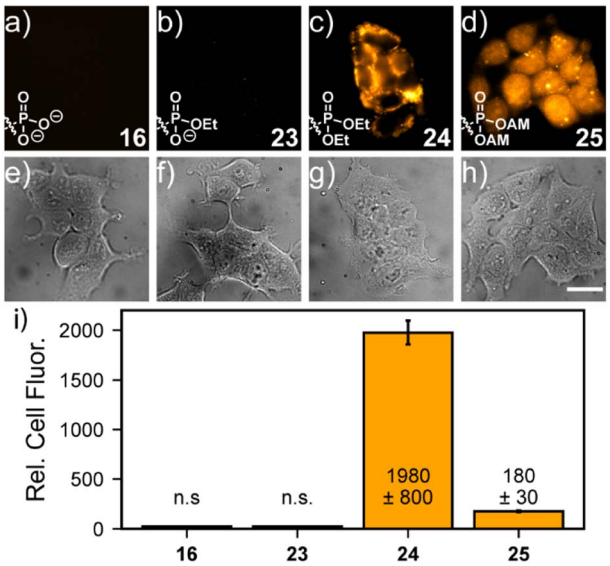

Fig. 2 Tunable localization of 3-phosphonoTMRs. Widefield fluorescence (a–d) and transmitted light (e–h) images of HEK293T cells stained with 500 nM dyes **16** (a and e), **23** (b and f), **24** (c and g), or **25** (d and h) in HBSS for 20 min at 37 °C. Quantification (i) of cellular fluorescence. Values are mean fluorescence intensity ± S.E.M. for $n = 21$, 32, 45, and 19 regions of interest (ROI) for each dye. Each ROI contained between 2 and 20 individual cells. "n.s." means that the cellular fluorescence values were not above background fluorescence. Coverslips were placed into fresh HBSS prior to imaging. Scale bar is 20 μm.

phosTMR·2OEt **24** (Fig. 2d and S8e–h†) or carboxyTMR AM (Fig. S9 and S10†). This is different from the behavior of the diethyl ester of phosTMR **24** and different from the behavior of the AM ester of traditional carboxyTMR, which localize to mitochondria (Fig. S9†). The differential cellular localization of **25** may stem from intracellular AM hydrolysis to yield phosTMR with a net negative charge (pK_{a2} 7.3); the greater charge density of phosTMR *vs.* carboxyTMR (net negative *vs.* net neutral at pH 7.4) likely precludes localization to the mitochondria.

phosTMR AM **25** also displays excellent cellular retention (Fig. S10a–c, g†). Serial washing of stained cells showed no decrease in the fluorescence intensity of **25**, up to 36 min after loading. On the other hand, after 3 washes carboxyTMR AM shows a 40% decrease in mitochondrial fluorescence intensity (Fig. S10d–f, g†), suggesting the additional negative charge provided by a 3-phosphonate enhances cellular retention.

Voltage sensing with phosphonorhodamines

The high water solubility, tunable cellular localization, and persistent anionic charge at physiological pH make phosTMR well-suited for voltage imaging applications, where retention of fluorophores on the extracellular surface of the plasma membrane is a critical feature. Rhodamine Voltage Reporters (RhoVRs) are a class of voltage sensing indicators that exhibit absorption and emission profiles in the green to orange regions of the visible spectrum. While voltage sensitive fluorophores typically rely on 3-sarcosine (RhoVR 1)[42] or 3-sulfonate (sRhoVR 1)[43] functionalities for membrane anchoring, expansion to a 3-phosphonate (phosRhoVRs) would allow us to take advantage of the scalability of the acid-free condensation chemistry.

Reaction of 5-bromo-2-phosphonobenzaldehyde **27** with 3-dimethylaminophenol in TFE, results in precipitation of triarylmethane **28** in quantitative yield (Fig. 3a). Dehydration and oxidation with chloranil gives conversion to the corresponding 6-bromo-3-phosphonotetramethyl rhodamine. This is a large

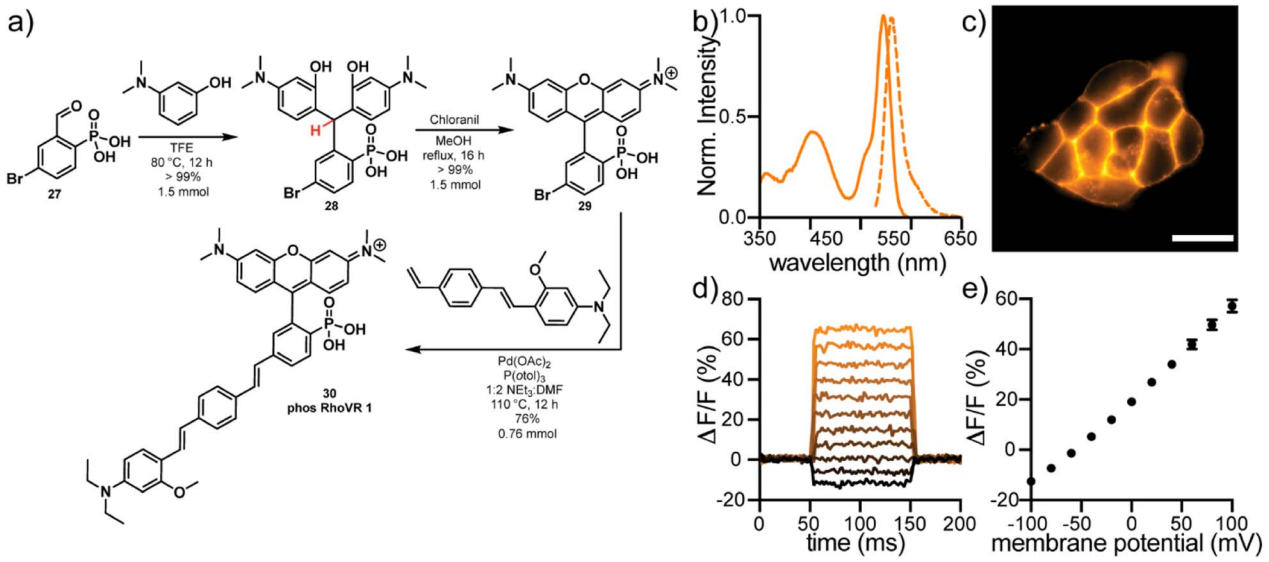

Fig. 3 Synthesis and characterization of phosRhoVR 1. (a) Synthesis of phosRhoVR 1, **30** from aldehyde **27**. (b) Normalized absorbance (solid line) and fluorescence emission (dashed line) spectra of phosRhoVR 1 in ethanol. (c) HEK cells stained with 500 nM phosRhoVR 1. Scale bar is 20 μm. (d) Plot of the fractional change in fluorescence of phosRhoVR 1 *vs.* time for 100 ms hyper- and depolarizing steps (±100 mV in 20 mV increments) for single HEK cells under whole-cell voltage-clamp mode. (e) Plot of $\Delta F/F$ *vs.* final membrane potential, revealing a voltage sensitivity of approximately 37% per 100 mV. Error bars are ±SEM for $n = 6$ cells. If not visible, error bars are smaller than the marker.

increase the in yield of the condensation to **29** (>99%) relative to the 3-carboxy (57%) and 3-sulfono (44%) analogs.[42,43] This reaction can be performed on at least a 1.5 mmol scale to furnish hundreds of milligrams of pure material without column chromatography.

Heck coupling of **29** to a phenylenevinylene molecular wire produces phosRhoVR 1, **30,** as a crude triethylamine salt which can be purified by reverse phase silica chromatography in 76% yield (0.76 mmol, 432 mg, Fig. 3a). In the comparable synthesis of the 3-amide analog, RhoVR 1, Heck coupling to the analogous 3-carboxytetramethylrhodamine is followed by a HATU coupling with *N*-Boc-sarcosine and TFA deprotection, resulting in a substantially lower 9% yield over 3 steps.[42] The streamlined and higher yielding synthesis of phosRhoVRs not only alleviates the time-consuming bottleneck in voltage reporter synthesis but also enables access to RhoVRs in much greater quantities (hundreds *vs.* tens of milligrams at a time).

phosRhoVR 1 displays characteristic absorption and emission profiles of 3-phosphono-tetramethylrhodamine, centered at 545 and 562 nm, respectively, with the addition of an absorption band at 402 nm from the molecular wire (Fig. 3b). In live HEK cells, fluorescence is localized primarily to the plasma membranes (Fig. 3c). The negatively charged phosphonate is sufficient to prevent internalization despite the positive charge of the rhodamine. phosRhoVR 1 shows a nearly 2-fold improvement in cellular brightness compared to RhoVR 1, when loaded under identical conditions (500 nM, Fig. S11†). Patch clamp electrophysiology coupled with fluorescence microscopy reveals a voltage sensitivity of 37% $\Delta F/F$ per 100 mV for phosRhoVR 1 (Fig. 3d and e), which is comparable but lower than the reported 47% for RhoVR 1 and 44% for sRhoVR 1.[42,43] However, given the improved cellular brightness, phosRhoVR 1 provides a nearly 2-fold increase in signal-to-noise for detecting membrane potential changes. PhosRhoVR 1 shows retention on the plasma membrane similar to RhoVR 1 (Fig. S12†). Both RhoVR 1 and phosRhoVR 1 are well-retained on the plasma membrane compared to di-4-ANEPPS, which shows some internalization after 30 minutes (Fig. S12†).

Conclusions

In summary, we report the synthesis of rhodamine fluorophores bearing 3-phosphonates *via* relatively mild chemistry. This chemistry relies on intramolecular aldehyde activation provided by the phosphonic acid functionality, negating the need for exogenous acid. Phosphonate substitution has little effect on photophysical properties of rhodamines but provides a 12× to 500× increase in water solubility compared to 3-carboxyTMR or 3-sulfonoTMR. PhosphonoTMRs are suitable for live-cell imaging. Intracellular delivery and retention of phosphonorhodamines can be controlled by esterification, and AM esters of phosphonorhodamines show differential localization, increased cell brightness, and improved retention compared to traditional carboxy analogs.

Additionally, 3-phosphonate functionality is readily incorporated into voltage sensing scaffolds. Fluorescent voltage reporters with a 3-phosphono group possess excellent voltage sensitivity, 2× improved cellular brightness, and can be synthesized in hundreds of milligram quantities. Future work will expand 3-phosphonate substitution to the entire family of xanthene fluorophores, including rhodols and other 10′ heteroatom substitutions.

Data availability

Data is included in ESI.†

Author contributions

JLT: conceptualization, investigation, formal analysis, visualization, original draft preparation, and review & editing, RPG: investigation, formal analysis, and review & editing, BRB: investigation, formal analysis, and review & editing, KMH: investigation, formal analysis, and review, SML: investigation, formal analysis, and review, EWM: conceptualization, funding acquisition, formal analysis, supervision, visualization, original draft preparation, and review & editing.

Conflicts of interest

There are no conflicts to declare.

Acknowledgements

E. W. M. acknowledges support from the Camille Dreyfus Teacher-Scholar Fellowship and the National Institute for General Medical Sciences (R35GM119855). B. R. D. was supported, in part, by a training grant from NIGMS (T32GM666098). S. M. L. was supported by a Graduate Research Fellowship from the National Science Foundation (DGE 2146752).

Notes and references

1 L. D. Lavis and R. T. Raines, Bright building blocks for chemical biology, *ACS Chem. Biol.*, 2014, **9**, 855–866.
2 L. D. Lavis and R. T. Raines, Bright ideas for chemical biology, *ACS Chem. Biol.*, 2008, **3**, 142–155.
3 M. Beija, C. A. M. Afonso and J. M. G. Martinho, Synthesis and applications of rhodamine derivatives as fluorescent probes, *Chem. Soc. Rev.*, 2009, **38**, 2410–2433.
4 T. Karstens and K. Kobs, Rhodamine B and rhodamine 101 as reference substances for fluorescence quantum yield measurements, *J. Phys. Chem.*, 2002, **84**, 1871–1872.
5 J. B. Grimm, B. P. English, J. Chen, J. P. Slaughter, Z. Zhang, A. Revyakin, R. Patel, J. J. Macklin, D. Normanno, R. H. Singer, T. Lionnet and L. D. Lavis, A general method to improve fluorophores for live-cell and single-molecule microscopy, *Nat. Methods*, 2015, **12**, 244–250.
6 J. B. Grimm, A. J. Sung, W. R. Legant, P. Hulamm, S. M. Matlosz, E. Betzig and L. D. Lavis, Carbofluoresceins and carborhodamines as scaffolds for high-contrast fluorogenic probes, *ACS Chem. Biol.*, 2013, **8**, 1303–1310.

7 J. B. Grimm, T. D. Gruber, G. Ortiz, T. A. Brown and L. D. Lavis, Virginia Orange: A Versatile, Red-Shifted Fluorescein Scaffold for Single- And Dual-Input Fluorogenic Probes, *Bioconjugate Chem.*, 2016, **27**, 474–480.
8 M. Fu, Y. Xiao, X. Qian, D. Zhao and Y. Xu, A design concept of long-wavelength fluorescent analogs of rhodamine dyes: replacement of oxygen with silicon atom, *Chem. Commun.*, 2008, 1780–1782.
9 K. Hirabayashi, K. Hanaoka, T. Takayanagi, Y. Toki, T. Egawa, M. Kamiya, T. Komatsu, T. Ueno, T. Terai, K. Yoshida, M. Uchiyama, T. Nagano and Y. Urano, Analysis of Chemical Equilibrium of Silicon-Substituted Fluorescein and Its Application to Develop a Scaffold for Red Fluorescent Probes, *Anal. Chem.*, 2015, **87**, 9061–9069.
10 J. B. Grimm, T. A. Brown, A. N. Tkachuk and L. D. Lavis, General Synthetic Method for Si-Fluoresceins and Si-Rhodamines, *ACS Cent. Sci.*, 2017, **3**, 975–985.
11 T. Egawa, Y. Koide, K. Hanaoka, T. Komatsu, T. Terai and T. Nagano, Development of a fluorescein analogue, TokyoMagenta, as a novel scaffold for fluorescence probes in red region, *Chem. Commun.*, 2011, **47**, 4162–4164.
12 X. Chai, X. Cui, B. Wang, F. Yang, Y. Cai, Q. Wu and T. Wang, Near-Infrared Phosphorus-Substituted Rhodamine with Emission Wavelength above 700 nm for Bioimaging, *Chem.–Eur. J.*, 2015, **21**, 16754–16758.
13 X. Zhou, R. Lai, J. R. Beck, H. Li and C. I. Stains, Nebraska Red: a phosphinate-based near-infrared fluorophore scaffold for chemical biology applications, *Chem. Commun.*, 2016, **52**, 12290–12293.
14 J. Liu, Y. Q. Sun, H. Zhang, H. Shi, Y. Shi and W. Guo, Sulfone-rhodamines: a new class of near-infrared fluorescent dyes for bioimaging, *ACS Appl. Mater. Interfaces*, 2016, **8**, 22953–22962.
15 L. V. Johnson, M. L. Walsh and L. B. Chen, Localization of mitochondria in living cells with rhodamine 123, *Proc. Natl. Acad. Sci. U. S. A.*, 1980, **77**, 990–994.
16 J. L. Turnbull, B. R. Benlian, R. P. Golden and E. W. Miller, Phosphonofluoresceins: Synthesis, Spectroscopy, and Applications, *J. Am. Chem. Soc.*, 2021, **143**, 6194–6201.
17 M. Ceresole, Verfahren zur Darstellung von Farbstoffen aus der Gruppe des Meta-amidophenol-Phtaleïns, *Ger. Pat.*, 44002, 1887.
18 T. Sandmeyer, Red dye, *US Pat.*, 573299, 1896.
19 M. Fu, X. Zhang, J. Wang, H. Chen and Y. Gao, Progress of Synthesis and Separation of Regioisomerically Pure 5(6)-Substituted Rhodamine, *Curr. Org. Chem.*, 2016, **20**, 1584–1590.
20 G. Mudd, I. P. Pi, N. Fethers, P. G. Dodd, O. R. Barbeau and M. Auer, A general synthetic route to isomerically pure functionalized rhodamine dyes, *Methods Appl. Fluoresc.*, 2015, **3**, 045002.
21 P. E. Deal, R. U. Kulkarni, S. H. Al-Abdullatif and E. W. Miller, Isomerically pure tetramethylrhodamine voltage reporters, *J. Am. Chem. Soc.*, 2016, **138**, 9085–9088.
22 S. J. Dwight and S. Levin, Scalable Regioselective Synthesis of Rhodamine Dyes, *Org. Lett.*, 2016, **18**, 5316–5319.
23 J. B. Grimm and L. D. Lavis, Synthesis of Rhodamines from Fluoresceins Using Pd-Catalyzed C–N Cross-Coupling, *Org. Lett.*, 2011, **13**, 6354–6357.
24 L. Wu and K. Burgess, Synthesis and Spectroscopic Properties of Rosamines with Cyclic Amine Substituents, *J. Org. Chem.*, 2008, **73**, 8711–8718.
25 G. Lukinavičius, K. Umezawa, N. Olivier, A. Honigmann, G. Yang, T. Plass, V. Mueller, L. Reymond, I. R. Corrêa Jr, Z.-G. Luo, C. Schultz, E. A. Lemke, P. Heppenstall, C. Eggeling, S. Manley and K. Johnsson, A near-infrared fluorophore for live-cell super-resolution microscopy of cellular proteins, *Nat. Chem.*, 2013, **5**, 132–139.
26 C. Fischer and C. Sparr, Direct Transformation of Esters into Heterocyclic Fluorophores, *Angew. Chem., Int. Ed.*, 2018, **57**, 2436–2440.
27 J. Kagan, The Structure of Phthalaldehydic Acid, *J. Org. Chem.*, 1967, **32**, 4060–4062.
28 A. Berkessel, J. A. Adrio, D. Hüttenhain and J. M. Neudörfl, Unveiling the 'booster effect' of fluorinated alcohol solvents: aggregation-induced conformational changes and cooperatively enhanced H-bonding, *J. Am. Chem. Soc.*, 2006, **128**, 8421–8426.
29 J. P. Bégué, D. Bonnet-Delpon and B. Crousse, Fluorinated Alcohols: A New Medium for Selective and Clean Reaction, *Synlett*, 2004, **2004**, 18–29.
30 S. Minegishi, S. Kobayashi and H. Mayr, Solvent Nucleophilicity, *J. Am. Chem. Soc.*, 2004, **126**, 5174–5181.
31 R. D. Franz, Comparisons of pK_a and log P values of some carboxylic and phosphonic acids: synthesis and measurement, *AAPS PharmSci*, 2001, **3**, E10.
32 T. Iwata, R. Kawano, T. Fukami and M. Shindo, Retro-Friedel-Crafts-Type Acidic Ring-Opening of Triptycenes: A New Synthetic Approach to Acenes, *Chem.–Eur. J.*, 2022, **28**, e202104160.
33 E. J. Goethals, E. H. Schacht, Y. E. Bogaert, S. I. Ali and Y. Tezuka, The polymerization of azetidines and azetidine derivatives, *Polym. J.*, 1980, **12**, 571–581.
34 R. Bandichhor, A. D. Petrescu, A. Vespa, A. B. Kier, F. Schroeder and K. Burgess, Synthesis of a new water-soluble rhodamine derivative and application to protein labeling and intracellular imaging, *Bioconjugate Chem.*, 2006, **17**, 1219–1225.
35 J. B. Grimm and L. D. Lavis, Caveat fluorophore: an insiders' guide to small-molecule fluorescent labels, *Nat. Methods*, 2022, **19**, 149–158.
36 N. Panchuk-Voloshina, R. P. Haugland, J. Bishop-Stewart, M. K. Bhalgat, P. J. Millard, F. Mao, W. Y. Leung and R. P. Haugland, Alexa dyes, a series of new fluorescent dyes that yield exceptionally bright, photostable conjugates, *J. Histochem. Cytochem.*, 1999, **47**, 1179–1188.
37 M. J. S. Dewar, 478. Colour and constitution. Part I. Basic dyes, *J. Chem. Soc.*, 1950, 2329–2334.
38 E. B. Knott, 227. The colour of organic compounds. Part I. A general colour rule, *J. Chem. Soc.*, 1951, 1024–1028.
39 R. Y. Tsien, A non-disruptive technique for loading calcium buffers and indicators into cells, *Nature*, 1981, **290**, 527–528.

40 L. D. Lavis, T.-Y. Chao and R. T. Raines, Synthesis and utility of fluorogenic acetoxymethyl ethers, *Chem. Sci.*, 2011, **2**, 521–530.

41 C. Schultz, M. Vajanaphanich, A. T. Harootunian, P. J. Sammak, K. E. Barrett and R. Y. Tsien, Acetoxymethyl esters of phosphates, enhancement of the permeability and potency of cAMP, *J. Biol. Chem.*, 1993, **268**, 6316–6322.

42 P. E. Deal, R. U. Kulkarni, S. H. Al-Abdullatif and E. W. Miller, Isomerically Pure Tetramethylrhodamine Voltage Reporters, *J. Am. Chem. Soc.*, 2016, **138**, 29.

43 R. U. Kulkarni, M. Vandenberghe, M. Thunemann, F. James, O. A. Andreassen, S. Djurovic, A. Devor and E. W. Miller, *In Vivo* Two-Photon Voltage Imaging with Sulfonated Rhodamine Dyes, *ACS Cent. Sci.*, 2018, **4**, 1371–1378.